

Article

Supramolecular Functionalities Influence the Thermal Properties, Interactions and Conductivity Behavior of Poly(ethylene glycol)/LiAsF₆ Blends

Jui-Hsu Wang ¹, Chih-Chia Cheng ¹, Oleksii Altukhov ², Feng-Chih Chang ^{1,2,*} and Shiao-Wei Kuo ^{2,*}

¹ Institute of Applied Chemistry, National Chiao Tung University, Hsinchu 30010, Taiwan;
E-Mails: gody.ac95g@nctu.edu.tw (J.-H.W.); chihchia.ac95g@nctu.edu.tw (C.-C.C.)

² Department of Materials and Optoelectronic Science, National Sun Yat-Sen University,
Kaohsiung 804, Taiwan; E-Mail: a.aleksey.v@gmail.com

* Authors to whom correspondence should be addressed; E-Mails: changfc@mail.nctu.edu.tw (F.-C.C.);
kuosw@faculty.nsysu.edu.tw (S.-W.K.); Tel./Fax: +886-7-525-4099 (S.-W.K.).

Received: 6 May 2013; in revised form: 20 June 2013 / Accepted: 20 June 2013 /

Published: 4 July 2013

Abstract: In this study, we tethered terminal uracil groups onto short-chain poly(ethylene glycol) (PEG) to form the polymers, uracil (U)-PEG and U-PEG-U. Through AC impedance measurements, we found that the conductivities of these polymers increased upon increasing the content of the lithium salt, LiAsF₆, until the Li-to-PEG ratio reached 1:4, with the conductivities of the LiAsF₆/U-PEG blends being greater than those of the LiAsF₆/U-PEG-U blends. The ionic conductivity of the LiAsF₆/U-PEG system reached as high as 7.81×10^{-4} S/cm at 30 °C. Differential scanning calorimetry, wide-angle X-ray scattering, ⁷Li nuclear magnetic resonance spectroscopy and Fourier transform infrared spectroscopy revealed that the presence of the uracil groups in the solid state electrolytes had a critical role in tuning the glass transition temperatures and facilitating the transfer of Li⁺ ions.

Keywords: supramolecular structure; multiple hydrogen bonding; polymer electrolytes

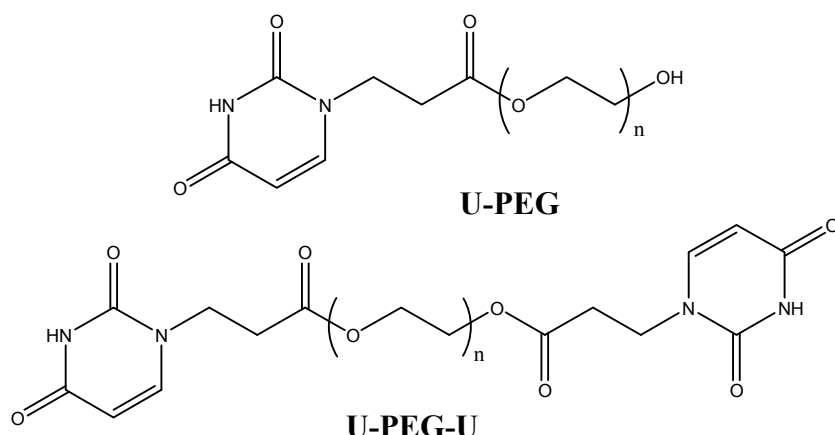
1. Introduction

A great concern regarding our possible future energy problems is the need to develop highly efficient and stable energy conversion systems. Polymer electrolytes, which have many potential applications in, for example, high-energy-density batteries and fuel cells, have been studied extensively during the past three decades [1–4]. Solid polymer electrolytes (SPEs), which are complexes of polymers and metal salts, can be prepared by dissolving salts in polar polymer hosts; they can then be applied in large-scale batteries [5–10]. In general, ionic transport occurs in the amorphous regions of such polymers as a result of coupling and segmental motion between the metal ions and the polar groups of the polymer. The interactions of Li⁺ ions within SPEs determine the properties and performance of their corresponding batteries. Obtaining relatively high Li⁺ ion conductivities in SPEs under ambient conditions, however, remains a challenge; in addition, greater understanding of the ionic interactions within SPEs will be necessary if we are to further improve ionic conductivities.

Poly(ethylene oxide) (PEO)-based polymeric electrolytes have been among the most extensively studied polymer ionic conductors, because their structures benefit rapid ion transport. PEOs exhibit relatively good complexation properties with ions, high flexibility and good mechanical stability at temperatures beyond their melting points. Unfortunately, a high content of their crystalline phases can limit the conductivity of PEO-based electrolytes [11–13]. Many research efforts aimed at enhancing the ionic conductivities of PEO-based SPEs have focused on suppressing their crystallinity through the incorporation of inorganic fillers (e.g., clays) to form composite polymeric electrolytes [14], through copolymerization of PEO with macromonomers [15] and through blending with other polymers [16]. In addition, much effort has been exerted toward enhancing the ionic conductivity of PEO-based electrolytes to appropriate levels under ambient conditions [17]. In previous studies, we focused on preparing solid state electrolytes based on PEO/D2000/LiClO₄/clay [18], PEO/PPBI/LiOTf [15], PEO/LiClO₄/phenolic resin [19] and LiClO₄/PEO/PCL [20]. In addition, we have also incorporated noncovalently interacting (multiple hydrogen bonding) functionalities into PEO polymer backbones to improve the properties of their SPEs [21,22]. Multiple hydrogen bonding interactions in supermolecules are moderately strong and highly directional, leading to their relating polymers possessing several attractive properties, including thermo-reversibility, responsiveness to external stimuli (e.g., pH, solvent polarity, temperature and concentration) and improved thermal stability relative to that of related single-hydrogen-bonding systems [23–25]. Recently, studies of specific structural organizations from oligomers modified with noncovalently interacting functionalities have been attracting increasing attention. In this present study, we developed a new type of SPE based on PEO oligomers tethered to noncovalently interacting functionalities. In a previous study, Wang *et al.* found that the ionic conductivity of short-chain PEO was higher than that of long-chain PEO [26]; although the short-chain PEO also possessed relatively low thermal and mechanical properties, they demonstrated that the incorporation of polar groups into the polyether chain could lead to improvements in ionic conductivity, as well as good electrochemical properties. The possibility of improving ionic conductivity further by increasing the polarity of the polymer host could be performed by adding polar functional groups onto the polymer backbone [27]. To improve the thermal and mechanical properties of short-chain PEO ($M = 350$ g/mol) without compromising its ionic conductivity, in this study, we tethered uracil (U), a self-complementary, noncovalently interacting functionality, to the chain ends of

poly(ethylene glycol) (PEG), forming U-PEG and U-PEG-U derivatives (Scheme 1). We then analyzed the ionic conductivities of lithium-based solid polymer films prepared from these U-based PEO derivatives and lithium hexafluoroarsenate (LiAsF_6) at various molar ratios. Using differential scanning calorimetry (DSC), wide-angle X-ray scattering (WAXS), AC impedance measurements, ^{7}Li nuclear magnetic resonance (NMR) spectroscopy and Fourier transform infrared (FTIR) spectroscopy, we characterized the thermal and crystalline properties, ionic conductivity and molecular interactions of these systems.

Scheme 1. Chemical Structures of uracil (U)-poly(ethylene glycol) (PEG) and U-PEG-U.



2. Experimental Section

2.1. Materials

Acrylate PEG ($M = 350$ g/mol) and methacrylate PEG ($M = 360$ g/mol) were obtained from Aldrich Chemical. Triethylamine was purchased from TEDIA. Acryloyl chloride and U were obtained from Acros. Lithium hexafluoroarsenate (LiAsF_6 ; Aldrich, St. Louis, MO, United States) was dried in a vacuum oven at $80\text{ }^{\circ}\text{C}$ for 24 h and stored in a desiccator prior to use. All solvents for high-performance liquid chromatography (HPLC) were obtained from TDCI. U-PEG [3-(2,4-dioxo-3,4-dihydro-2*H*-pyrimidin-1-yl)propionic acid 2-hydroxyethyl ester] and U-PEG-U [3-(2,4-dioxo-3,4-dihydro-2*H*-pyrimidin-1-yl)propionic acid 2-[4-(2,4-dioxo-3,4-dihydro-2*H*-pyrimidin-1-yl)-2-oxobutoxy]ethyl ester] were prepared through Michael additions using previously reported procedures [28]. A solution of PEG acrylate, U and potassium *tert*-butoxide in DMSO in a flask equipped with a condenser was heated on a hot plate ($60\text{ }^{\circ}\text{C}$) for 48 h. After distillation of the DMSO, the solid residue was dissolved in CH_2Cl_2 and filtered. The solvent was evaporated from the filtrate in a rotary evaporator; the residue was dried under vacuum for 24 h to yield U-PEG. A solution of acryloyl chloride in THF was added through a dropping funnel into a solution of PEG acrylate, triethylamine and THF in a 500 mL flask, cooled in an ice bath, and then the mixture was stirred for 24 h. The precursor—collected after centrifugation, filtration and rotary evaporation of the solvent—was added to a flask containing a solution of U and potassium *tert*-butoxide in DMSO, and then the stirred mixture was heated at $60\text{ }^{\circ}\text{C}$ for 48 h. After distillation of the DMSO, the solid residue was dissolved in CH_2Cl_2 , filtered and concentrated to give the final product, which was dried under vacuum for 24 h to yield U-PEG-U.

2.2. LiAsF₆/U-PEG and LiAsF₆/U-PEG-U Polymer Electrolytes

The blending molar ratios of Li⁺ ions to the total oxygen atom contents of the ethylene oxide units in each PEG main chain were used to identify the formed Li/U-PEG or Li/U-PEG-U blends. All samples were dissolved in DMF and stirred for 24 h. The solutions were cast onto Teflon dishes and maintained at 80 °C for 24 h to remove the solvent; the dishes were then further dried under vacuum at 80 °C for an additional 48 h. To prevent contact with the air and moisture, the polymer electrolytes were transferred to a glove box under a N₂ atmosphere.

2.3. Characterization

¹H-NMR spectra were recorded using a Varian Unity Inova 300 FT NMR spectrometer (McKinley Scientific, Sparta, NJ, USA) operated at 500 MHz; chemical shifts are reported in parts per million (ppm). Molecular weights and molecular weight distributions were determined through gel permeation chromatography (GPC) using a Waters 510 HPLC equipped with a 410 differential refractometer (Milford, MA, USA), a refractive index (RI) detector and three Ultrastyragel columns (100, 500 and 1000) connected in series of increasing pore size (eluent: DMF-*d*₇; flow rate: 0.6 mL·min⁻¹). FTIR spectra (KBr disk method) were measured using a Nicolet Avatar 320 FTIR spectrometer (Thermo Scientific, Waltham, MA, USA); 32 scans were collected at a resolution of 1 cm⁻¹. The sample chamber was purged with N₂ to maintain film dryness. Thermal analyses were performed using a DSC instrument (TA Instruments Q-20, New Castle, DE, USA). The sample (*ca.* 4–6 mg) was weighed and sealed in an aluminum pan. The glass transition temperatures (*T_g*) were taken as the midpoints of the heat capacity transitions between the upper and lower points of deviation from the extrapolated glass and liquid lines, at a scan rate of 20 °C min⁻¹ over a temperature range from −50 to −150 °C. WAXS measurements were performed using a BL17A1 wiggler beamline at the National Synchrotron Radiation Research Center (NSRRC), Taiwan. AC impedance was measured using a Princeton Applied Research VersaStat 4 potentiostat (Oak Ridge, TN, USA), with a frequency range from 10 μHz to 10 MHz and a maximum current of up to 1 A with additional booster options ranging from 2 to 20 A. The potentiostatic method (scan frequency from 100,000 to 1 Hz; amplitude: 10) was used to obtain the total resistance from the Nyquist plot. The conductivity (σ) of the samples in the longitudinal direction was calculated using the relationship:

$$\sigma = \frac{L}{(R \times d \times W)} \quad (1)$$

where *L* is the distance between the electrodes and *d* and *W* are the thickness and width of the sample stripe, respectively. The value of *R* was derived from the low intersect of the high frequency semi-circle on a complex impedance plane with the Re(*Z*)-axis. Solid state ⁷Li magic angle spinning (MAS) NMR spectra were recorded at 300 K using a Bruker DSX-400 NMR spectrometer equipped with a 7 mm double-resonance probe, operated at 400.13 MHz for ¹H nuclei and 155.27 MHz for ⁷Li nuclei; typical experimental conditions: π/2 duration, 2 μs; recycle delay, 8 s; ¹H decoupling power, 65 kHz; spinning speed, 2 kHz; 1 M aqueous LiCl solution was used as an external chemical shift reference (0 ppm).

3. Results and Discussion

3.1. Thermal Analyses

According to the results of a previous study [28], we knew that the properties of polymer/salt mixtures can be changed dramatically as a result of ionic aggregation. Here, we first performed thermal analyses to determine whether the properties of these systems were affected by the addition of the lithium salt. Figure 1 presents DSC traces of the LiAsF₆/U-PEG and LiAsF₆/U-PEG-U polymer electrolytes and the changes in the values of T_g at different contents of LiAsF₆. As mentioned in our previous report [28], acrylate-PEG is a crystalline oligomer having values of T_g , T_c , and T_m of -70 °C, -51 °C, and -5 °C, respectively. Addition of the U groups to the PEG derivative caused U-PEG and U-PEG-U to become amorphous, with their values of T_g increasing to -34 and -23 °C, respectively. These data indicate that adding U—a noncovalently interacting functional group that experiences self-complementary interactions—to PEG disrupted the polymer's chain folding and decreased its crystallinity. The values of T_g of U-PEG and U-PEG-U increased upon increasing the content of the salt LiAsF₆, until the Li-to-PEG molar ratio reached 1:4 in each case. The ionic interactions or ionic clusters formed in the amorphous regime of the ionomers usually resemble physical cross-linking. The mobility of the polymer chains is restricted through such physical cross-linking, thereby leading to higher glass transition temperatures relative to that of the mother polymer. In general, the value of T_g increased gradually upon the addition of the salt as a result of an increased number of ion-polymer and ion-ion interactions, with a maximum glass transition temperature achieved at a certain content of the lithium salt; above the optimized lithium salt content, the value of T_g tended to decrease as a result of greater interchain distances [29].

Kim *et al.* proposed an extended configuration entropy model to predict the glass transition temperatures of polymer/salt complex systems [30]. They employed the equation:

$$\ln \frac{T_{g12}}{T_{g1}} = \beta \left[(1 - \gamma_{12} \ln(\frac{z-1}{e})) (\frac{\phi_1}{r_1} \ln \phi_1 + \frac{\phi_2}{r_2} \ln \phi_2) - \frac{\phi_2}{r_2 v m} \frac{4}{3} A_{diss} I_{3/2} \tau(I^{1/2}) \right] \quad (2)$$

where T_{g1} and T_{g12} are the glass transition temperatures of the pure polymer and the polymer/salt blend, respectively, and ϕ_i and r_i are the volume fraction and the degree of polymerization for component i, respectively ($r_2 = 1$). The value of β is determined using the equation:

$$\beta = zR / M_{1u} \Delta C_{pp} \quad (3)$$

where z is the lattice coordination number, R is the gas constant, M_{1u} is the molecular weight of the repeating unit of the polymer and ΔC_{pp} is the isobaric specific heat of the polymer. The term, r_{12} , is a proportionality constant representing the strength of the interaction between the polymer and the salt. The term:

$$\frac{\phi_2}{r_2 v m} \frac{4}{3} A_{diss} I_{3/2} \tau(I^{1/2}) = A^{DH} \quad (4)$$

accounts for the cation-anion interaction. Table 1 lists the molecular weights, values of T_g , specific heats and densities of the components tested in this study. Figure 2 presents the variation in the value of T_g as a function of the lithium salt content; the solid lines, calculated from Equation (1), reveal that a

good correlation exists between the experimental data and the model's predictions for both the U-PEG and U-PEG-U systems at relatively low lithium salt contents. Larger deviations appeared at higher lithium salt contents; in this case, however, the value of A^{DH} should be constant in the U-PEG and U-PEG-U systems, because they feature the same lithium salt [31]. Nevertheless, if we take into account only the strength of the interaction parameter, that for the lithium salt/U-PEG-U blend ($r_{12} = 2.7$; $A^{DH} = 0.02$) would be greater than that for the lithium salt/U-PEG blend ($r_{12} = 2.6$; $A^{DH} = 0.02$), indicating that the stronger interactions are those between the lithium salt and U-PEG-U. Defunctionalization with two U groups may result in more intermolecular interactions with the lithium salt relative to that obtained with only mono-functionalized U groups in the PEG matrix.

Figure 1. Differential scanning calorimetry (DSC) thermograms of (a) LiAsF₆/U-PEG and (b) LiAsF₆/U-PEG-U blends.

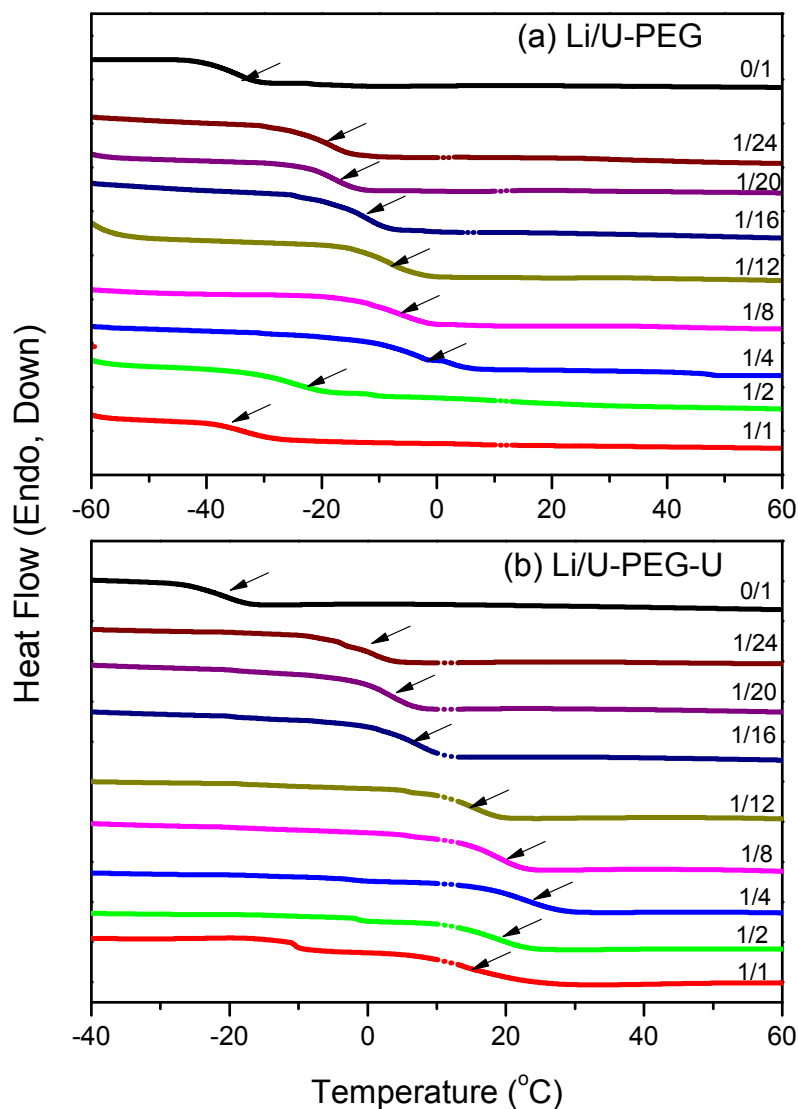
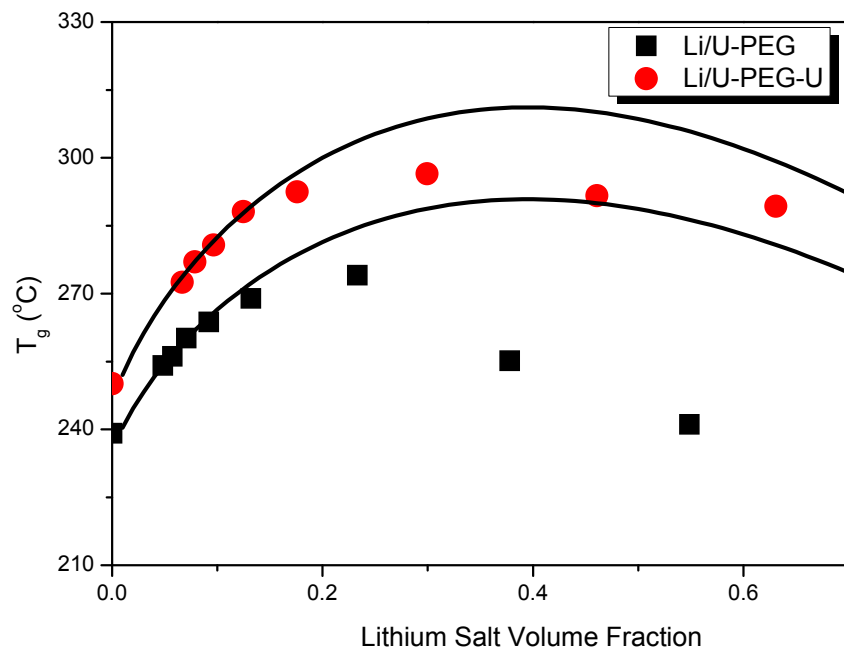


Table 1. Molecular weights, values of T_g , specific heats and densities of the components used in this study.

Polymers	M (g/mol)	T_g (°C)	ΔC_{pp} [J/(kg K)] ^a	Density (g/cm ³)
U-PEG	465	-34	1,261	1.368 ^a
U-PEG-U	647	-23	1,261	1.374 ^a
LiAsF ₆	196	—	—	2.252
Blend System	z	β	r_{12}	A^{DH}
LiAsF ₆ /U-PEG	6	0.899	2.6	0.02
LiAsF ₆ /U-PEG-U	6	0.899	2.7	0.02

Notes: ^a Values obtained using the group contribution method [32].

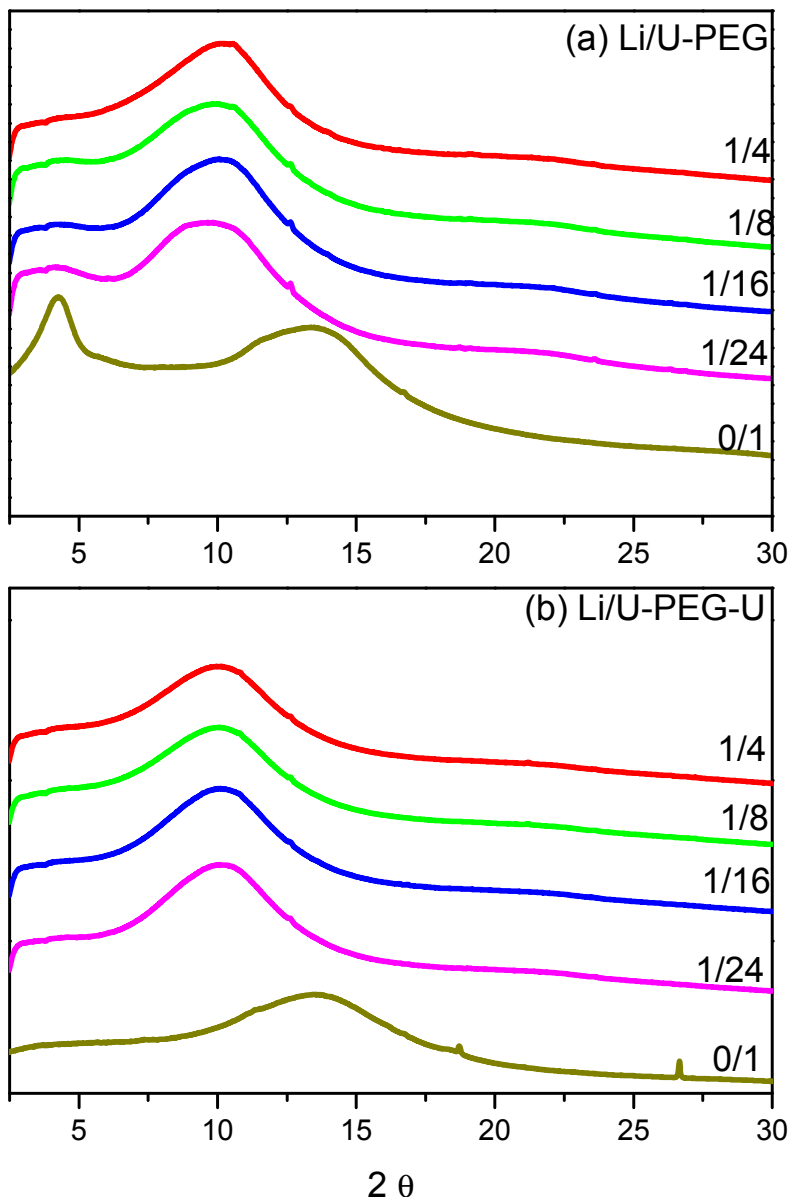
Figure 2. Values of T_g for U-PEG and U-PEG-U blends incorporating various lithium salt contents. Solid lines were calculated from the configuration entropy model.



3.2. WAXD Analyses

Figure 3 displays WAXD patterns of the LiAsF₆/U-PEG and LiAsF₆/U-PEG-U polymer electrolyte systems. For U-PEG, we observe characteristic peaks at 4.2° and 13.5°, corresponding to structures constructed by U units and an amorphous halo, respectively. In contrast, U-PEG-U underwent supramolecular polymerization, resulting in only one characteristic peak, attributable to its amorphous halo. Upon increasing the concentration of salt added to both U-PEG and U-PEG-U, the signals for their amorphous halos underwent obvious shifts to the left, indicating that the *d*-spacings for the lithium salt/U-PEG and U-PEG-U blends increased accordingly as a result of the coordination of Li⁺ ions to the polymer chain through ion-dipole interactions, with the AsF₆⁻ anions weakly solvated and distributed among the polymer chains. These large solvated AsF₆⁻ anions led to chain expansion, forcing the polymer chains apart; a similar phenomenon had been observed for a LiClO₄/PPO complex [33].

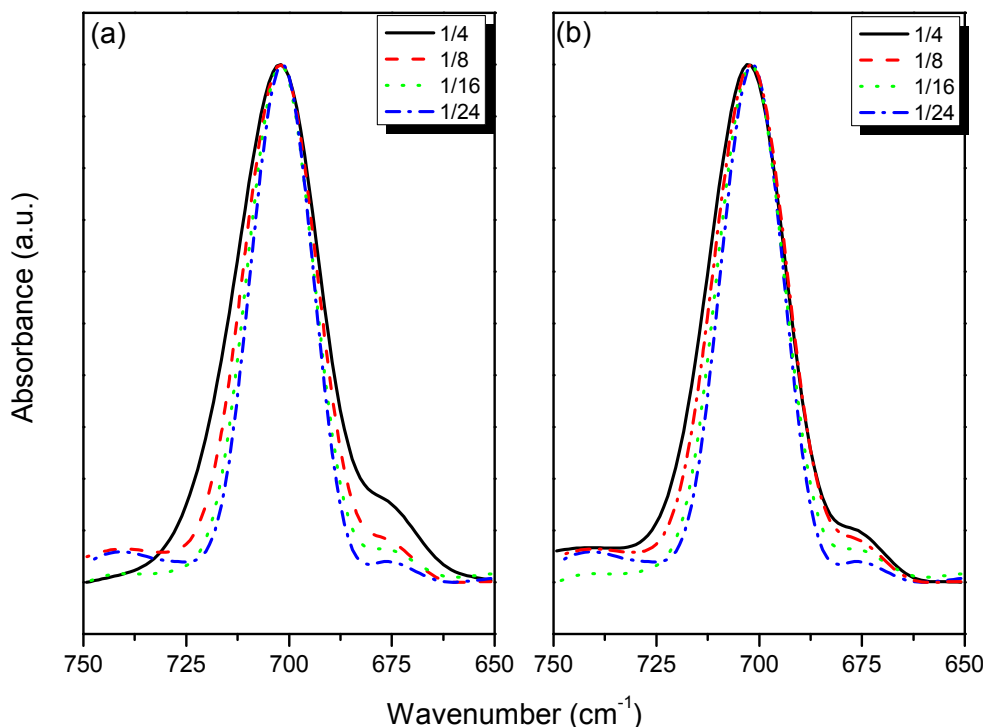
Figure 3. WAXD spectra of (a) LiAsF₆/U-PEG and (b) LiAsF₆/U-PEG-U blends at room temperature.



3.3. FTIR Spectroscopic Analyses

Figure 4 presents FTIR spectra of the LiAsF₆/U-PEG and LiAsF₆/U-PEG-U systems in range from 640 to 740 cm⁻¹. Peaks at 702 cm⁻¹, 717 cm⁻¹ and 676 cm⁻¹ correspond to the free ions, contact ion pairs and a combination of the ν_5 and ν_6 modes of AsF₆⁻, respectively [34]. The intensity of the band at 676 cm⁻¹ increased upon increasing the lithium salt content in both the U-PEG and U-PEG-U systems. The band at 702 cm⁻¹, representing free ions, shifted the higher wavenumber upon increasing the content of the lithium salt; a slight shoulder appeared at 717 cm⁻¹ as a result of the formation of contact ion pairs, indicating that ionic aggregation occurred at relatively high lithium salt contents. Nevertheless, almost all of the lithium salts adopted the form of free ions in the U-PEG and U-PEG-U matrices; for example, the area percentage of free ions, determined through curve fitting, was approximately 87.5% at a relatively high lithium salt content (LiAsF₆-to-U-PEG molar ratio of 1:4).

Figure 4. FTIR spectra (from 750 to 650 cm^{-1}) of (a) LiAsF₆/U-PEG and (b) LiAsF₆/U-PEG-U blends at room temperature.



Next, we turned our attention to other infrared absorption peaks as probes, with and without the addition of the lithium salt. Figure 5 displays scale-expanded FTIR spectra of the lithium salt/U-PEG and lithium salt/U-PEG-U blends in the region featuring the ether vibrational modes (1000–1200 cm^{-1}). The spectra of pure U-PEG and U-PEG-U featured characteristic bands at 1107 cm^{-1} and 1104 cm^{-1} , respectively, corresponding to the C–O–C ether absorptions of the PEG units. Upon the formation of ionic bonds between the lithium salt and PEG (at Li-to-U-PEG and Li-to-U-PEG-U molar ratios of 1:1), these bands shifted to 1092 cm^{-1} and 1100 cm^{-1} , respectively. The much larger shift for the Li/U-PEG blend ($\Delta\nu = 15 \text{ cm}^{-1}$) relative to that for the Li/U-PEG-U blend ($\Delta\nu = 4 \text{ cm}^{-1}$) indicates that the lithium salt interacts with U-PEG stronger than the U-PEG-U system in this study.

Figure 6 displays scale-expanded FTIR spectra of the lithium salt/U-PEG and lithium salt/U-PEG-U blends in the region featuring the C=O vibration modes (1600–1800 cm^{-1}). For both pure U-PEG and U-PEG-U, we observe five major peaks representing (i) the free C=O groups from the acrylate units of U-PEG (1734 cm^{-1}) and U-PEG-U (1729 cm^{-1}); (ii) the free C₂=O groups from the U units of U-PEG and U-PEG-U (1706 cm^{-1}); (iii) the free C₄=O groups from the U units of U-PEG (1684 cm^{-1}) and U-PEG-U (1680 cm^{-1}); (iv) the multiply hydrogen-bonded C₄=O groups of the U units of U-PEG (1662 cm^{-1}) and U-PEG-U (1652 cm^{-1}); and (v) the double bonds in the U rings of U-PEG and U-PEG-U (1621 cm^{-1}) [35]. Scheme 2a,c summarizes the peak assignments of U-PEG and U-PEG-U. The wavenumbers for the signals for the U-PEG-U system were slightly lower than those for the U-PEG system, as would be expected, because of the greater possibility of forming hydrogen bonds in the former. For the LiAsF₆/U-PEG system (Figure 6a), the intensity of each peak did not change significantly upon increasing the lithium salt content, until the Li-to-U-PEG ratio reached 1:8. In general, the highest

conductivity and T_g behavior occurs in most cases at a Li-to-PEG ratio of 1:8, indicating that the lithium salt interacts almost entirely with the ether groups at molar ratios lower than 1:8 [17–19,36]. In this study, we found, however, that the highest T_g behavior occurred at a Li-to-PEG ratio of 1:4, presumably because the U and acrylate groups in the U-PEG system also had inter-association ability at relatively high lithium salt contents. The signals in the spectra in Figure 6a had different shapes at Li-to-U-PEG ratios of 1:4 and 1:1, with significant new peaks at 1710 and 1680 cm^{-1} , corresponding to the ionic bonds between the lithium salt and the C=O groups of the acrylate and U ($\text{C}_2=\text{O}$) units of U-PEG, respectively. Furthermore, the signals for the free acrylate C=O (1729 cm^{-1}) and multiply hydrogen-bonded C=O (1655 cm^{-1}) groups of U-PEG were slightly shifted as a result of changes to their chemical environments upon increasing the lithium salt content, as revealed in Scheme 2b. We observed similar phenomena for the LiAsF₆/U-PEG-U system (Figure 6b), with the signal for the free acrylate C=O group shifting from 1729 to 1726 cm^{-1} upon increasing the Li-to-U-PEG-U ratio to 1:1. A new absorption peak appeared, however, at 1672 cm^{-1} , corresponding to the C=O groups of U units ($\text{C}_2=\text{O}$) of U-PEG-U ionically bonded to the lithium salt, Li-to-U-PEG-U molar ratios of less than 1:8; this wavenumber is lower than that for the same ionic bond in Li/U-PEG, as would be expected. Further increasing the Li-to-U-PEG-U ratio to 1:4 and 1:1 resulted in broad spectral features, similar to those in the spectra of the Li/U-PEG systems, indicating the existence of more complicated chemical environments.

Figure 5. FTIR spectra (from 1200 to 1000 cm^{-1}) of (a) LiAsF₆/U-PEG and (b) LiAsF₆/U-PEG-U blends at room temperature.

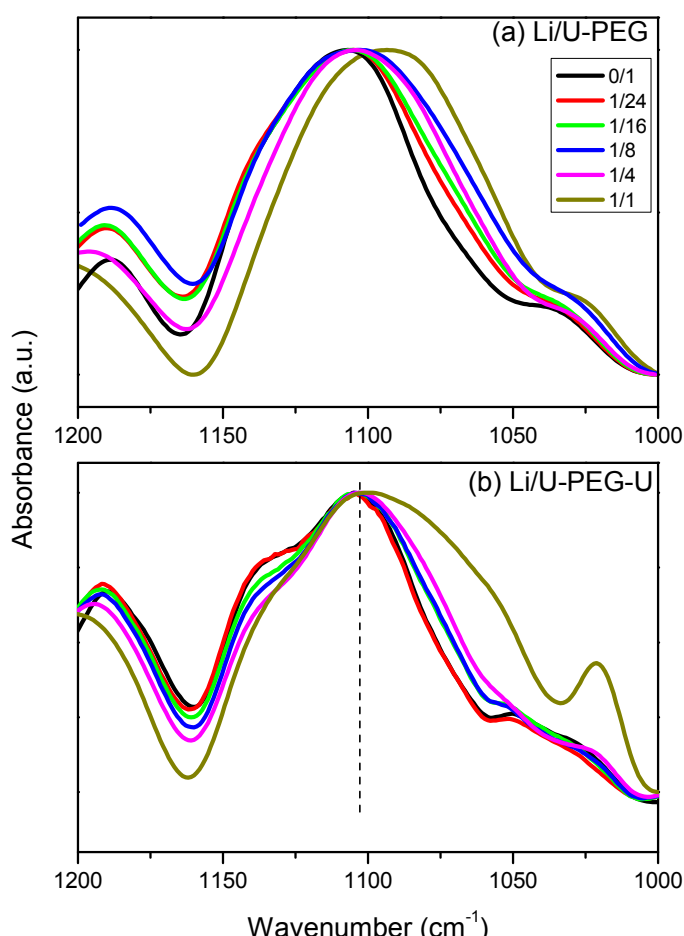
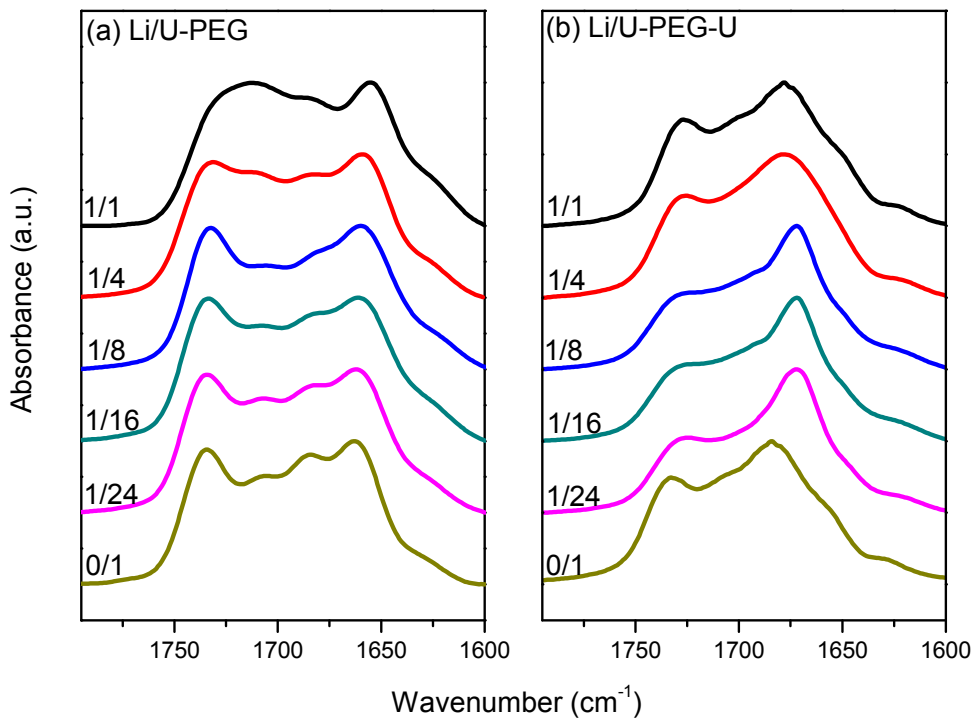
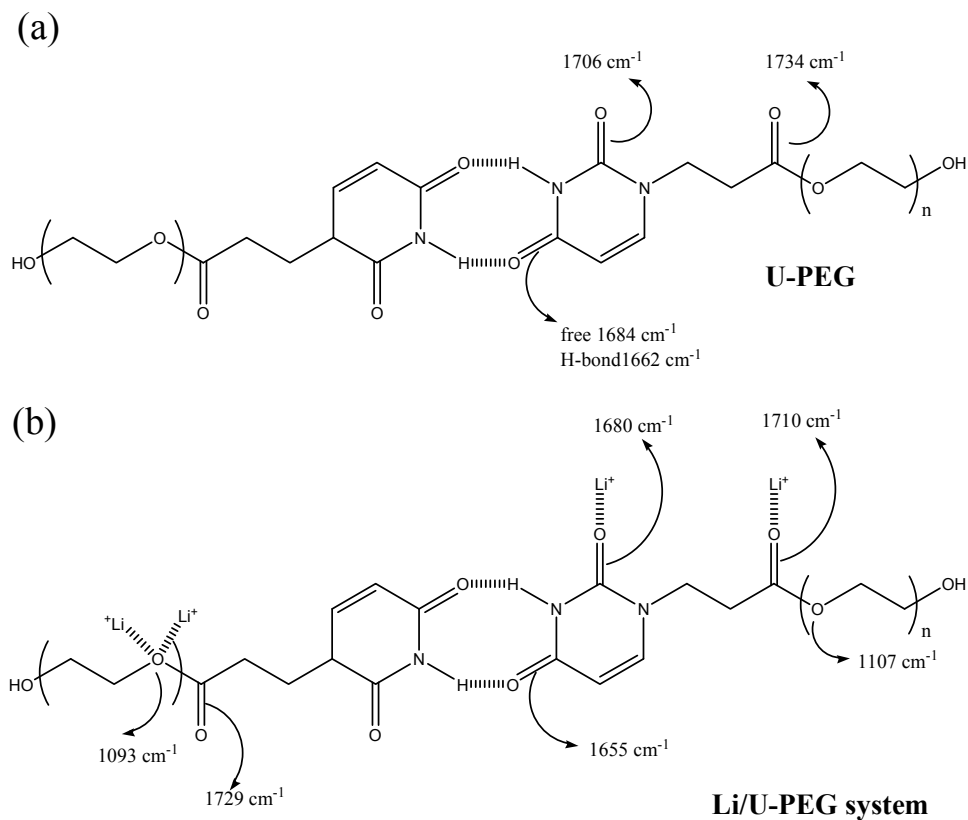


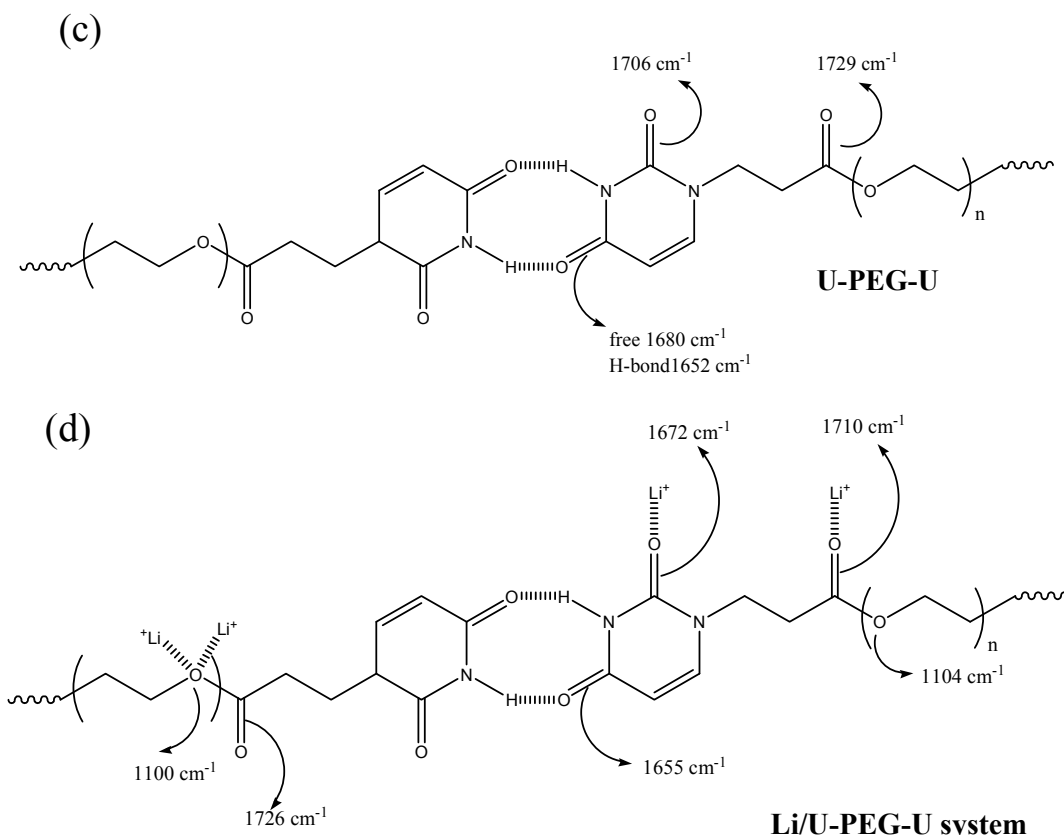
Figure 6. FTIR spectra (from 1800 to 1600 cm^{-1}) of (a) LiAsF₆/U-PEG and (b) LiAsF₆/U-PEG-U blends at room temperature.



Scheme 2. Peak assignments in the spectra of (a) U-PEG; (b) Li/U-PEG blends; (c) U-PEG-U; (d) Li/U-PEG-U blends.



Scheme 2. Cont.



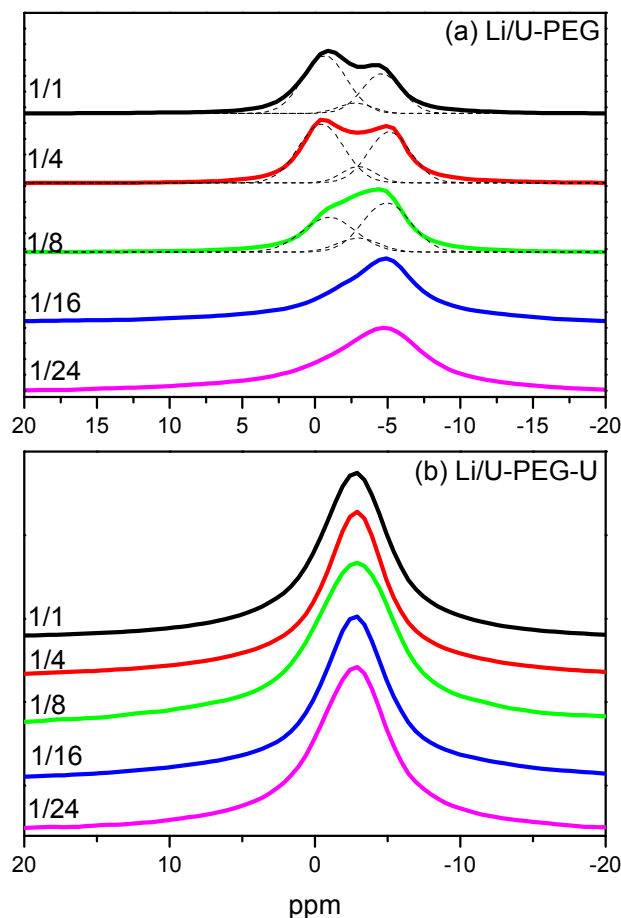
3.4. ^7Li MAS NMR Spectroscopy

Solid state ^7Li -NMR spectroscopy is used widely to study the interactions between Li^+ ions and polymer hosts [37–39], because the strong receptivity of the Li^+ ion makes it a very attractive analytical tool. Figure 7 presents ^7Li NMR spectra, recorded at 300 K, of the lithium salt/U-PEG and lithium salt/U-PEG-U blends. For the Li/U-PEG system, only a single peak (peak I) appears for the blends at lower lithium salt contents (Li-to-PEG ratios of 1:24 and 1:16); we assign this peak, at high field (*ca.* –4.8 ppm), to represent the interaction between the ether groups of PEG and the Li^+ cation. Further increasing the lithium salt content, we observed two new peaks near –2.76 (peak II) and –0.36 (peak III) ppm, based on curve fitting results (Figure 7a). For the Li/U-PEG-U system, only a single peak near –2.76 ppm (peak II) appeared for the blends at any lithium salt content; its position did not change upon increasing the Li^+ ion content. We would expect that a greater possibility to interact with the C=O groups would induce a downfield shift upon increasing the content of the lithium salt [20]. Based on the results of our FTIR spectroscopic analyses, we assigned peak II to represent the interaction between the C=O groups of the U units of U-PEG and the Li^+ cations and peak III to the interaction between the C=O groups of the acrylate units of U-PEG and the Li^+ cations. The fraction of peak III increased upon increasing the lithium salt content in the Li/U-PEG system, as revealed in Figure 7a, consistent with the FTIR spectroscopic analyses in Figure 6.

Based on these FTIR and ^7Li solid state NMR spectroscopic analyses, we found that the lithium salt adopted almost a free ionic state at a Li-to-PEG molar ratio of less than 1:8. For the Li/U-PEG system, the lithium salt preferred to interact with the ether groups of U-PEG at Li-to-U-PEG molar ratios of

less than 1:8, but then interacted with the C=O groups of the acrylate and U units of U-PEG at higher lithium salt contents. For the Li/U-PEG-U system, the lithium salt interacted with both the ether and C=O groups of U-PEG-U at any lithium salt content. Thus, the lithium salt had much greater ability to interact with the ether groups in the Li/U-PEG system than those in the Li/U-PEG-U system.

Figure 7. Solid state ^{7}Li proton-decoupled MAS NMR spectra of (a) LiAsF₆/U-PEG and (b) LiAsF₆/U-PEG-U blends at room temperature.



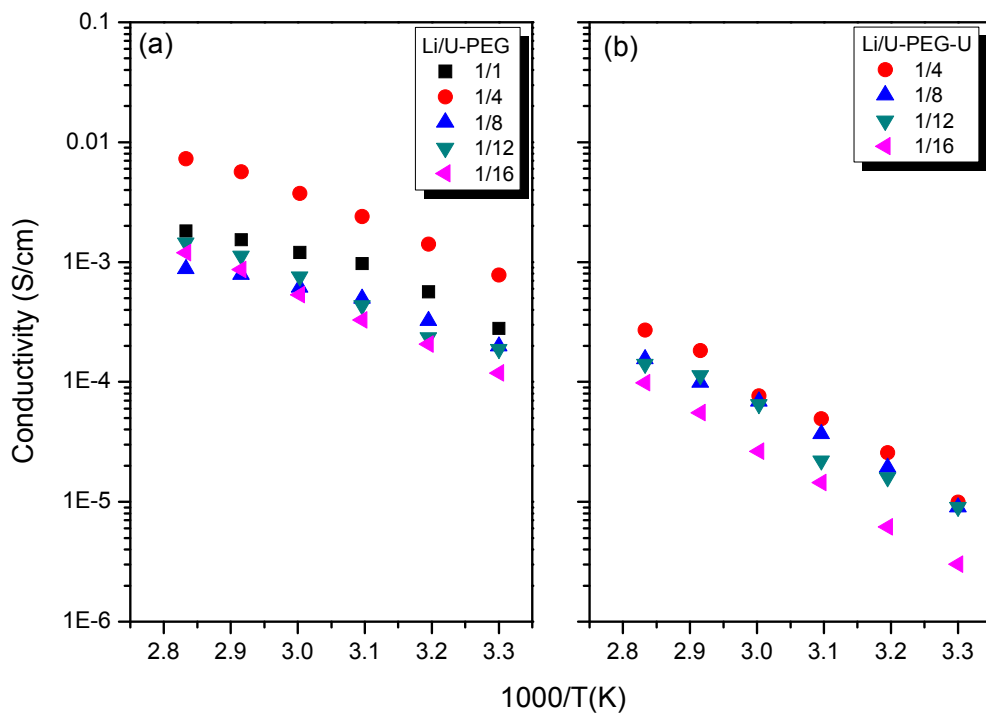
3.5. Ionic Conductivity

Figure 8 presents ionic conductivity data for the LiAsF₆/U-PEG and LiAsF₆/U-PEG-U systems. The ionic conductivities of the LiAsF₆/U-PEG system were substantially higher than those of the LiAsF₆/U-PEG-U system at the same Li-to-PEG molar ratio. The highest ionic conductivity (7.81×10^{-4} S/cm at 30 °C) was that of the LiAsF₆/U-PEG system at a molar ratio of 1:4 (Figure 8a). In contrast, the LiAsF₆/U-PEG-U system did not exhibit improved ionic conductivities, even though it featured relatively more U groups. Figure 8b reveals that all of the LiAsF₆/U-PEG-U systems exhibited ionic conductivities of less than 1×10^{-5} S/cm. The Li/U-PEG-U system possessed the highest conductivity at a molar ratio of 1:24 (3.01×10^{-6} S/cm at 30 °C). The ionic conductivity (σ) of an electrolyte is defined as the product of the concentration of the ionic charge carries and their mobility:

$$\sigma = \sum_i n_i u_i z_i \quad (5)$$

where n_i , z_i , and u_i refer to the number of charge carriers, the ionic charge and the ionic mobility, respectively. The FTIR and Li⁷-NMR spectra revealed that the free anions produced more charge carriers (higher n_i); more free charge carriers increased the ionic mobility, because they disrupted the strong intra-association between the Li⁺ cations and the anions. Therefore, we would expect the conductivity to increase. For the LiAsF₆/U-PEG blends, appropriate values of T_g , specific structures derived from the U groups and association between the Li⁺ ions and U units suggest that they are potential solid state electrolyte materials. Although the LiAsF₆/U-PEG-U system possessed relatively higher fractions of U units within their blends, supramolecular polymerization resulted in relatively high values of T_g and affected association between the Li⁺ ions and U groups, leading to relatively low ionic conductivity. Acrylate-PEG systems at the same lithium salt content exhibit a substantially lower values of T_g and behaves as liquid-like materials; in contrast, the U-PEG systems exhibited relatively high ionic conductivities, indicating that the U groups of U-PEG play a critical role in ion transfer. These U units cannot only construct specific structures, but also facilitate ion transfer [40]. In addition, although the U-PEG-U systems featured relatively higher U contents, they exhibited lower ionic conductivity, because of the decreased flexibility of the structures formed through supramolecular polymerization mediated by the U units.

Figure 8. Ionic conductivity plotted with respect to temperature for (a) LiAsF₆/U-PEG and (b) LiAsF₆/U-PEG-U blends.



4. Conclusions

We have prepared a new solid state electrolyte material comprising U-PEG and LiAsF₆. These LiAsF₆/U-PEG blends possess appropriate values of T_g and ionic conductivities for practical applications; for example, the LiAsF₆/U-PEG blend at a molar ratio of 1:4 possessed an ionic conductivity of 7.81×10^{-4} S/cm at 30 °C. These blends have potential use as solid state electrolytes in

secondary lithium batteries. We have found that the U groups in this solid state electrolyte play a critical role in tuning the values of T_g and facilitating Li^+ ion transfer.

Acknowledgments

This study was supported financially by the National Science Council, Taiwan, Republic of China, under contracts NSC 100-2221-E-110-029-MY3 and NSC 101-2628-E-110-003.

Conflict of Interest

The authors declare no conflict of interest.

References

1. Ye, Y.S.; Huang, Y.J.; Cheng, C.C.; Chang, F.C. A new supramolecular sulfonated polyimide for use in proton exchange membranes for fuel cells. *Chem. Commun.* **2010**, *46*, 7554–7556.
2. Ye, Y.S.; Yen, Y.C.; Cheng, C.C.; Chen, W.Y.; Tsai, L.T.; Chang, F.C. Sulfonated poly(ether ether ketone) membranes crosslinked with sulfonic acid containing benzoxazine monomer as proton exchange membranes. *Polymer* **2009**, *50*, 3196–3203.
3. Saikia, D.; Wu, H.Y.; Lin, C.P.; Pan, Y.C.; Fang, J.; Tsai, L.D.; Fey, G.T.K.; Kao, H.M. New highly conductive organic-inorganic hybrid electrolytes based on star-branched silica based architectures. *Polymer* **2012**, *53*, 6008–6020.
4. Murata, K.; Izuchi, S.; Yoshihisa, Y. An overview of the research and development of solid polymer electrolyte batteries. *Electrochim. Acta* **2000**, *45*, 1501–1508.
5. Croce, F.; Appetecchi, G.B.; Persi, L. Nanocomposite polymer electrolytes for lithium batteries. *Nature* **1998**, *394*, 456–458.
6. Zhang, H.; Kullarni, S.; Wnder, S.L. Polyethylene glycol functionalized polyoctahedral silsesquioxanes as electrolytes for lithium batteries, fuel cells, and energy conversion. *J. Electrochem. Soc.* **2006**, *153*, A239–A248.
7. Lin, C.K.; Wu, I.D. Investigating the effect of interaction behavior on the ionic conductivity of Polyester/LiClO₄ blend systems. *Polymer* **2011**, *52*, 4106–4113.
8. Chiu, C.Y.; Yen, Y.J.; Kuo, S.W.; Chen, H.W.; Chang, F.C. Complicated phase behavior and ionic conductivities of PVP-*co*-PMMA based polymer electrolytes. *Polymer* **2007**, *48*, 1329–1342.
9. Pivovar, B.S. An overview of electro-osmosis in fuel cell polymer electrolytes. *Polymer* **2006**, *47*, 4194–4202.
10. Xue, C.C.; Meador, M.A.B.; Zhu, Z.; Ge, J.J.; Cheng, S.Z.D.; Putthanarat, S. Morphology of PI-PEO block copolymers for lithium batteries. *Polymer* **2006**, *47*, 6149–6155.
11. Xi, J.; Qiu, X.; Zheng, S.; Tang, X. Nanocomposite polymer electrolyte comprising PEO/LiClO₄ and solid super acid: Effect of sulphated-zirconia on the crystallization kinetics of PEO. *Polymer* **2005**, *46*, 5702–5706.
12. Rocco, A.M.; Carias, A.D.; Pereira, R.P. Polymer electrolytes based on a ternary miscible blend of poly(ethylene oxide), poly(bisphenol A-*co*-epichlorohydrin) and poly(vinyl ethyl ether). *Polymer* **2010**, *51*, 5151–5164.

13. Zardalids, G.; Ioannou, E.; Pispas, S.; Floudas, G. Relating structure, viscoelasticity, and local mobility to conductivity in PEO/LiTf electrolytes. *Macromolecules* **2013**, *46*, 2705–2714.
14. Berthier, C.; Gorecki, W.; Minier, M.; Armand, M.B.; Chabagno, J.M.; Rigaud, P. Microscopic investigation of ionic conductivity in alkali metal salts-poly(ethylene oxide) adducts. *Solid State Ion.* **1983**, *11*, 91–95.
15. Chen, H.W.; Chiu, C.Y.; Wu, H.D.; Shen, I.W.; Chang, F.C. Solid-state electrolyte nanocomposites based on poly(ethylene oxide), poly(oxypropylene) diamine, mineral clay and lithium perchlorate. *Polymer* **2002**, *43*, 5011–5016.
16. Xia, D.W.; Smid, J. Solid polymer electrolyte complexes of polymethacrylates carrying pendant oligo-oxyethylene(glyme) chains. *J. Polym. Sci. Polym. Lett. Ed.* **1984**, *22*, 617–621.
17. Li, J.; Khan, I.M. Highly conductive solid polymer electrolytes prepared by blending high molecular weight poly(ethylene oxide), poly(2- or 4-vinylpyridine), and lithium perchlorate. *Macromolecules* **1993**, *26*, 4544–4550.
18. Wieczorek, W.; Such, K.; Zalewska, A.; Raducha, D.; Florjanczyk, Z.; Stevens, J.R. Composite polyether electrolytes with Lewis acid type additives. *J. Phys. Chem. B* **1998**, *102*, 352–360.
19. Chen, H.W.; Xu, H.; Huang, C.F.; Chang, F.C. Novel polymer electrolyte composed of poly(ethylene oxide), lithium triflate, and benzimidazole. *J. Appl. Polym. Sci.* **2004**, *91*, 719–725.
20. Chen, H.W.; Jiang, C.H.; Wu, H.D.; Chang, F.C. Hydrogen bonding effect on the poly(ethylene oxide), phenolic resin, and lithium perchlorate-based solid-state electrolyte. *J. Appl. Polym. Sci.* **2004**, *91*, 1207–1216.
21. Chiu, C.Y.; Chen, H.W.; Kuo, S.W.; Huang, C.F.; Chang, F.C. Investigating the effect of miscibility on the ionic conductivity of LiClO₄/PEO/PCL ternary blends. *Macromolecules* **2004**, *37*, 8424–8430.
22. Yen, Y.C.; Cheng, C.C.; Kuo, S.W.; Chang, F.C. A new poly(amide urethane) solid state electrolyte containing supramolecular structure. *Macromolecules* **2010**, *43*, 2634–2637.
23. Sijbesma, R.P.; Meijer, E.W. Self-assembly of well-defined structures by hydrogen bonding. *Curr. Opin. Colloid Interface Sci.* **1999**, *4*, 24–32.
24. Elemans, J.A.; Rowan, A.E.; Nolte, R.J.M. Mastering molecular matter: Supramolecular architectures by hierarchical self-assembly. *J. Mater. Chem.* **2003**, *13*, 2661–2670.
25. Whitesides, G.M.; Grzybowski, B. Self-assembly at all scales. *Science* **2002**, *295*, 2418–2421.
26. Wang, Y.J.; Pan, Y.; Wang, L.; Pang, M.J.; Chen, L. Characterization of (PEO)LiClO₄-Li_{1.3}Al_{0.3}Ti_{1.7}(PO₄)₃ composite polymer electrolytes with different molecular weights of PEO. *J. Appl. Polym. Sci.* **2006**, *102*, 4269–4275.
27. Xu, W.; Belieres, J.P.; Angell, C.A. Ionic conductivity and electrochemical stability of poly[oligo(ethylene glycol)oxalate]-lithium salt complexes. *Chem. Mater.* **2001**, *13*, 575–580.
28. Wang, J.H.; Altukhov, O.; Cheng, C.C.; Chang, F.C.; Kuo, S.W. Supramolecular structures of uracil-functionalized PEG with multi-diamidopyridine POSS through complementary hydrogen bonding interactions. *Soft Matter* **2013**, *9*, 5196–5206.
29. Eisenberg, A.; Rinaudo, M. Polyelectrolytes and ionomers. *Polym. Bull.* **1990**, *24*, 671.
30. Kim, J.H.; Min, B.R.; Kim, C.K.; Won, J.; Kang, Y.S. New insights into the coordination mode of silver ions dissolved in poly(2-ethyl-2-oxazoline) and its relation to facilitated olefin transport. *Macromolecules* **2002**, *35*, 5250–5255.

31. Kim, J.H.; Min, B.R.; Won, J.; Kang, Y.S. Analysis of the glass transition behavior of polymer-salt complexes: An extended configurational entropy model. *J. Phys. Chem. B* **2003**, *107*, 5901–5905.
32. Koh, J.H.; Park, J.T.; Koh, J.K.; Kim, J.H. Prediction of the glass transition temperature of semicrystalline polymer/salt complexes. *J. Polym. Sci. B Polym. Phys.* **2009**, *47*, 793–798.
33. Kuo, S.W.; Wu, C.H.; Chang, F.C. Thermal properties, interactions, morphologies, and conductivity behavior in blends of poly(vinylpyridine)s and zinc perchlorate. *Macromolecules* **2004**, *37*, 192–200.
34. Carlsson, P.; Mattsson, B.; Swenson, J.; Borjesson, L.; Torell, L.M.; McGreevy, R.L.; Howell, W.S. Intermediate range structural correlations in polymer electrolyte PPO-LiClO₄ from neutron diffraction experiments and reverse Monte Carlo simulations. *Electrochim. Acta* **1998**, *43*, 1545–1550.
35. Deng, Z.; Irish, D.E. A Raman spectral study of solvation and ion association in the systems LiAsF₆/CH₃CO₂CH₃ and LiAsF₆/HCO₂CH₃. *Can. J. Chem.* **1991**, *69*, 1766–1773.
36. Meyer, F.; Raquez, J.M.; Verge, P.; de Arenaze, I.M.; Coto, B.; Voort, P.V.D.; Meaurio, E.; Dervaux, B.; Sarasua, J.R.; Prez, F.D.; *et al.* Poly(ethylene oxide)-*b*-poly(l-lactide) diblock copolymer/carbon nanotube-based nanocomposites: LiCl as supramolecular structure-directing agent. *Biomacromolecules* **2011**, *12*, 4086–4094.
37. Szekrenyes, Z.; Kamara, K.; Tarczay, G.; Pallas, A.L.; Marangoni, T.; Prato, M.; Bonifazi, D.; Bjork, J.; Hanke, F.; Persson, M. Melting of hydrogen bonds in uracil derivatives probed by infrared spectroscopy and ab initio molecular dynamics. *J. Phys. Chem. B* **2012**, *116*, 4626–4633.
38. Fu, R.; Ma, Z.; Zheng, J.P.; Au, G.; Plichta, E.J.; Ye, C. High-resolution ⁷Li solid-state NMR study of Li_xV₂O₅ cathode electrodes for Li-rechargeable batteries. *J. Phys. Chem. B* **2003**, *107*, 9730–9735.
39. Wang, H.L.; Kao, H.M.; Wen, T.C. Direct ⁷Li-NMR spectral evidence for different Li⁺ local environments in a polyether poly(urethane urea) electrolyte. *Macromolecules* **2000**, *33*, 6910–6912.
40. Dai, Y.; Wang, Y.; Greenbaum, S.G.; Bajue, S.A.; Golodnitsky, D.; Ardel, G.; Strauss, E.; Peled, E. Electrical, thermal and NMR investigation of composite solid electrolytes based on PEO, LiI and high surface area inorganic oxides. *Electrochim. Acta* **1998**, *43*, 1557–1561.

© 2013 by the authors; licensee MDPI, Basel, Switzerland. This article is an open access article distributed under the terms and conditions of the Creative Commons Attribution license (<http://creativecommons.org/licenses/by/3.0/>).